

Phase transition in the *ABC* model

M. Clincy,¹ B. Derrida,² and M. R. Evans¹¹*School of Physics, University of Edinburgh, Mayfield Road, Edinburgh EH9 3JZ, United Kingdom*²*Laboratoire de Physique Statistique de l'Ecole Normale Supérieure, 24 Rue Lhomond, 75231 Paris Cedex 05, France*

(Received 30 September 2002; revised manuscript received 27 February 2003; published 26 June 2003)

Recent studies have shown that one-dimensional driven systems can exhibit phase separation even if the dynamics is governed by local rules. The *ABC* model, which comprises three particle species that diffuse asymmetrically around a ring, shows anomalous coarsening into a phase separated steady state. In the limiting case in which the dynamics is symmetric and the parameter q describing the asymmetry tends to one, no phase separation occurs and the steady state of the system is disordered. In the present work, we consider the weak asymmetry regime $q = \exp(-\beta/N)$, where N is the system size, and study how the disordered state is approached. In the case of equal densities, we find that the system exhibits a second-order phase transition at some nonzero β_c . The value of $\beta_c = 2\pi\sqrt{3}$ and the optimal profiles can be obtained by writing the exact large deviation functional. For nonequal densities, we write down mean-field equations and analyze some of their predictions.

DOI: 10.1103/PhysRevE.67.066115

PACS number(s): 64.60.Cn, 02.70.Uu, 05.50.+q

I. INTRODUCTION

Nonequilibrium steady states, wherein the properties of a system are stationary but the steady state probabilities are not described by Boltzmann weights with respect to a local energy function, may exhibit a number of interesting phenomena absent from equilibrium systems: for example, driven diffusive systems [1] have generically long-range correlations; phase transitions may also occur in one-dimensional nonequilibrium steady states although they are, of course, precluded from one-dimensional equilibrium systems with short-range interactions.

Examples of nonequilibrium phase transitions include the absorbing state phase transitions [2] and the boundary-induced phase transitions in driven systems wherein a conserved current is driven through a finite open system [3–7]. Bulk (i.e., not boundary-driven) phase transitions may arise in systems with no absorbing states such as conserving driven systems through the introduction of several species of particles [8–13].

Phase separation has been exhibited in several one dimensional driven systems [8,14,15] consisting of several species of particles with nearest neighbor exchanges occurring with prescribed rates. Models in this class are the *ABC* model [14], the *AHR* model [8,9,16]—both containing three species of particles—and the *LR* model [15] which consists of two sublattices with two species each. The phase separation in these models has the striking feature of the domains of each species being pure. That is, far away from the domain walls, there is zero probability of finding a particle of one species in a domain of a different species. This is referred to as strong phase separation.

An understanding of this phenomenon has emerged through the exact solution of the steady state in some special cases of the *ABC* [14] and the *LR* models [15]. Even though the dynamics is strictly local, in these special cases it has been shown that the steady state obeys detailed balance with respect to a long-range energy function. The long-range interaction leads to superextensivity of this energy function,

i.e., the energy of most microscopic configurations scales quadratically with system size N so that the contribution of the entropy becomes negligible. Almost all configurations are therefore suppressed and only strongly phase separated configurations contribute. Although, generally, in the *ABC* and the *LR* models for nonequal numbers of particles detailed balance does not hold and one does not have an energy function, the same strong phase separation is observed in simulations [14].

In the *ABC* model, there is a parameter q that governs the local dynamics. It describes the asymmetry in the rates of nearest neighbor particle exchanges (see Sec. II). If $q < 1$ is held fixed, then one always has strong phase separation in the thermodynamic limit ($N \rightarrow \infty$). However for $q = 1$, in which case the particles exchange symmetrically, the system is in a homogeneous disordered state where all configurations are equally probable. In the present work, we investigate the *ABC* model in the weak asymmetry regime. That is, we introduce a system size dependence into q so that an extensive energy is recovered (when an energy function indeed exists). It turns out that the appropriate choice of q is

$$q = \exp\left(-\frac{\beta}{N}\right). \quad (1)$$

Thus, β is now the control parameter and plays the role of an inverse temperature, i.e., $\beta = 1/T$. In this regime, an interesting question arises as to how the transition from the strongly phase separated state to the disordered state occurs as T is varied. Since the energy function is of long range, it is possible to have a phase transition at a well-defined temperature $T_c = \beta_c^{-1}$ even though the system is one dimensional (1D) (phase transitions, in fact, do occur in one-dimensional systems with algebraically decaying interaction [17] or in the Bernasconi model [18] which is an Ising spin model with energy function given by long-range, four-spin interactions [19]).

In the present paper, we first summarize in Sec. II some known facts about the *ABC* model. In Sec. III, we present

our results of Monte Carlo simulations done in the weak asymmetry regime for an equal number of particles of each species. These simulations indicate that there is a critical value $\beta_c = 1/T_c \approx 11$. In Sec. IV, we derive the exact free energy functional for an arbitrary density profile from the expression for the weights in the steady state in the case of equal particle numbers. By minimizing this functional we obtain the exact value of $\beta_c = 2\pi\sqrt{3} \approx 10.88 \dots$ and the shape of the density profiles in the neighborhood of the transition. In Sec. V, we investigate the case of arbitrary global densities within a mean-field approximation. We observe that this approximation turns out to be exact in the case of equal numbers of particles.

II. THE ABC MODEL

The ABC model is defined on a 1D ring with N lattice sites. Each site is occupied by one of the three types of particles denoted as A , B , or C . They exhibit hard-core interaction, i.e. only one particle per site is allowed. Neighboring sites on the ring are exchanged according to the following rates:



Thus, for $q \neq 1$ the particles diffuse asymmetrically around the ring and in the case $q=1$ they diffuse symmetrically. Note that periodic boundary conditions are implied and the dynamics conserves the number of particles.

This model has been extensively studied in Ref. [14] by analytical and numerical means. Let us summarize in this section the main results. Starting from an initially random configuration, the system coarsens into a strongly phase separated state for any $q \neq 1$. Thus, the steady state exhibits long-range order, even though the dynamics is strictly local. We will restrict our discussion of $q \neq 1$ to the case $q < 1$ for simplicity. (The case $q > 1$ can be obtained by the transformation $q \rightarrow 1/q$ together with the exchange of A and B particles.) For $q=1$, particles of all species have equivalent dynamics, which results in a steady state in which all configurations have equal weight and the steady state of the system is disordered.

To understand the coarsening dynamics for $q < 1$, note that domain walls of the type BA , CB , and AC are unstable to interchanges leading to AB , BC , and CA , respectively. Therefore, A particles are driven to the left in a B domain and to the right in a C domain (particles B and C are also driven in other species domains). Thus the system arrives at a metastable configuration of the form $A \dots AB \dots BC \dots CA \dots AB \dots BC \dots CA \dots$ and a slow coarsening process, involving the elimination of the smallest domains, ensues. For ex-

ample, the time it takes an A particle to traverse a B domain of length l is of the order of q^l . Thus, the elimination of domains of size l occurs at a rate of order q^{-l} which results in the typical domain size growing as $l \sim \ln t$. This growth law which is slower than any power of t is referred to as anomalous coarsening [20]. Ultimately, the coarsening process results in a strongly phase separated state comprising three pure domains.

The general steady state is not, as yet, known. In the special case of equal particle numbers $N_A = N_B = N_C = N/3$, however, one can show that the steady state obeys detailed balance with respect to a long-range energy function \mathcal{H} . A configuration of the system is specified by the set of indicator variables $\{X_i\} = \{A_i, B_i, C_i\}$ which take value 1 or 0 depending on whether site i is occupied by the relevant particle or not. For example, $A_i = 1$ if site i is occupied by an A particle. Clearly, these variables satisfy $A_i + B_i + C_i = 1$. With these indicator variables, the energy function may be written as

$$\mathcal{H}(\{X_i\}) = \frac{1}{N} \sum_{i=1}^N \sum_{k=1}^{N-1} k(B_i C_{i+k} + C_i A_{i+k} + A_i B_{i+k}) \quad (5)$$

and the steady state weights of the system are given by

$$P(\{X_i\}) = Z_N^{-1} q^{\mathcal{H}(\{X_i\})}, \quad (6)$$

where $Z_N = \sum q^{\mathcal{H}(\{X_i\})}$ denotes the partition function. Note that the energy given in Ref. [14] differs by a constant from Eq. (5).

In Eq. (5), the interaction between sites i and $i+k$ are both long range and asymmetric, and the energy function is superextensive and scales quadratically with system size N .

The width of the domain walls in the phase separated state is of the order of $1/|\ln q|$ [14]. So for $q \rightarrow 1$, the size of the domain walls diverges and the system will be in a homogeneous disordered state. Moreover, we expect an interesting regime to occur when the width of the domain walls is of the order of the domain lengths $N/3$, i.e.,

$$\frac{1}{|\ln q|} \sim O(N). \quad (7)$$

This yields the weakly asymmetric regime stated in the Introduction, Eq. (1), where the control parameter is now $T = 1/\beta$. The steady state weight (5) and (6) also confirms that Eq. (1) is the natural choice for a scaling variable, since under this scaling (6) becomes

$$P_N(\{X_i\}) = Z_N^{-1} \exp[-\beta E_N(\{X_i\})], \quad (8)$$

where Z_N is a normalization constant (the partition function), and the extensive rescaled energy $E_N(\{X_i\})$ is defined as

$$E_N(\{X_i\}) = \mathcal{H}(\{X_i\})/N. \quad (9)$$

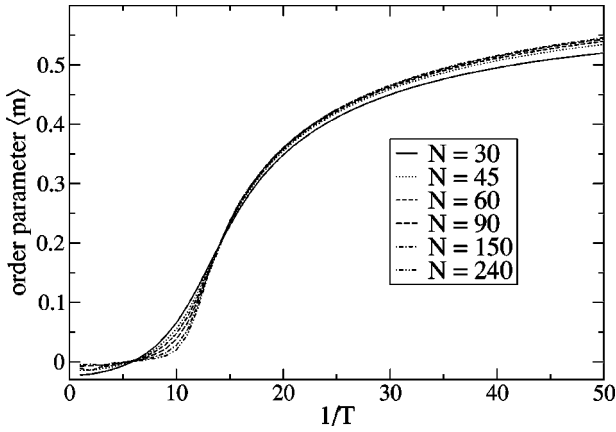


FIG. 1. Parameter m defined by Eq. (11) for system sizes $N = 30$ –240.

III. MONTE CARLO SIMULATIONS

We have measured by Monte Carlo simulations the number of nearest neighbor pairs of sites occupied by the same species of particles in the steady state. We shall refer to these as nearest neighbor (nn) matching pairs. For a completely disordered system (i.e., for $\beta=0$), the probability of finding a nn matching pair is $1/3$ for large N . As β increases, one expects this number to increase and to be equal to 1 as $\beta \rightarrow \infty$ (i.e., as one reaches the strongly separated regime).

In Fig. 1, we show the results of our simulations for m_N defined as

$$m_N = \frac{\text{(number of nn matching pairs)}}{\text{(system size)}} - \frac{1}{3} \quad (10)$$

$$= \frac{1}{N} \sum_{i=1}^N [A_i A_{i+1} + B_i B_{i+1} + C_i C_{i+1}] - \frac{1}{3}, \quad (11)$$

with the occupation variable $X_i = A_i, B_i, C_i$ defined as in Eq. (5). Note that because of the periodic boundary conditions, site $N+1$ is identified with site 1. We see that as N increases, m_N seems to be closer and closer to zero as $\beta < 11$, whereas it seems to have a well-defined limit m which depends on β for $\beta > 11$,

$$m = \lim_{N \rightarrow \infty} m_N. \quad (12)$$

Note that m only contains nearest neighbor correlations as opposed to, e.g., the measure of order used in Ref. [14] which contains long-range terms. Also one could consider the lowest Fourier mode of the density profile (see Sec. IV).

For $T < T_c$, we expect $0 < m < 2/3$, with m approaching $2/3$ in the limit $T \rightarrow 0$. This behavior can be seen in Fig. 1. For $1/T \approx 11$, a crossover from an ordered to a disordered state appears, which becomes sharper with the increasing system size. In Fig. 2, we plot the specific heat defined as $C_N = \partial E_N / \partial T$. One sees strong finite size effects at $\beta = 1/T \approx 11$. Moreover, the curves suggest that a discontinuity emerges in the infinite system limit which would be consistent with a second-order phase transition.

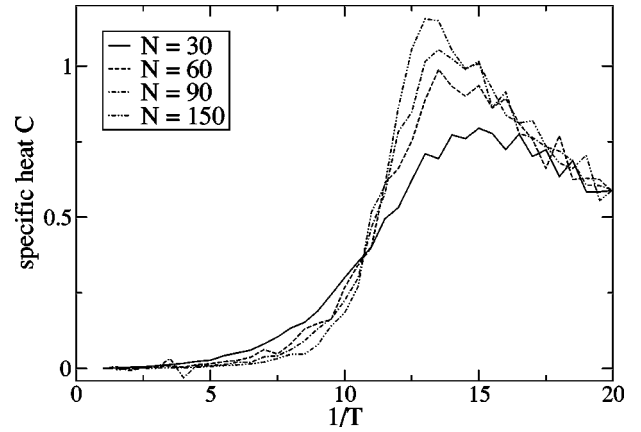


FIG. 2. Specific heat for system sizes $N = 30, 60, 90$, and 150 .

To determine the critical temperature of the system, we have performed a standard finite size scaling analysis [21] based on the distribution of the parameter m_N defined as in Eq. (11). Such an analysis has already proved to be effective in the study of nonequilibrium steady states [22,23]. We performed Monte Carlo simulations of the model for system sizes $N = 30$ to 210 over 10^9 sweeps in the steady state for each set of parameters. To determine the critical temperature T_c , we measured the ratio between two moments of the parameter m_N ,

$$U_N = 1 - \frac{\langle m_N^4 \rangle}{3 \langle m_N^2 \rangle^2}. \quad (13)$$

(In fact, since one does not have to distinguish between positive and negative values of the parameter m , the ratio $\langle m^2 \rangle / \langle m \rangle^2$ could as well be used to determine the critical temperature.)

At the critical temperature T_c , U_N has a universal value U^* . Thus, on measuring U_N for various system sizes as a function of T , U^* is the common intersection point of the curves and identifies T_c . Our results shown in Fig. 3 indicate $\beta_c = 1/T_c \approx 10.95$.

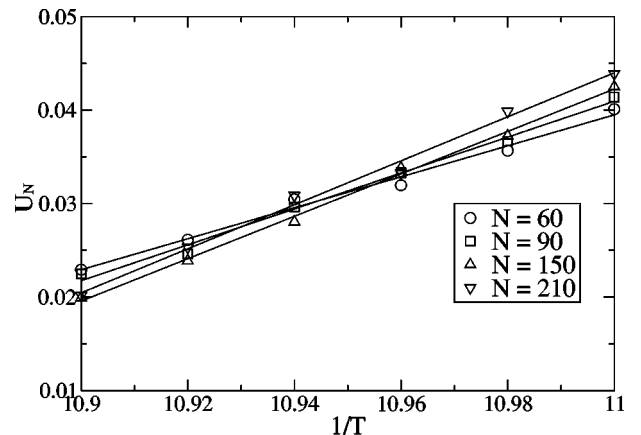


FIG. 3. Critical temperature T_c as an intersection point U^* of the fourth-order cumulant of the order parameter U_N (the straight lines are linear fits to the data).

IV. LARGE DEVIATION FUNCTIONAL FOR EQUAL DENSITIES AND THE EXACT TRANSITION TEMPERATURE

In this section, we consider only the case of equal numbers of each species

$$N_A = N_B = N_C = \frac{N}{3}, \quad (14)$$

where there exists an energy function given by Eqs. (5) and (9),

$$E_N(\{X_i\}) = \frac{1}{N^2} \sum_{i=1}^{N-1} \sum_{k=1}^{N-1} k(B_i C_{i+k} + C_i A_{i+k} + A_i B_{i+k}), \quad (15)$$

with the occupation variables $\{X_i\} = \{A_i, B_i, C_i\}$ defined as in Eq. (5). The steady state probabilities of the system are given by Eq. (8).

We pass to the continuum limit where $\rho_A(x), \rho_B(x)$, and $\rho_C(x)$ are the density profiles of A, B , and C particles, respectively, at position $x = i/N$. Then, the free energy functional [24,25] (or large deviation functional) $\mathcal{F}[\rho_A(x), \rho_B(x), \rho_C(x)]$ which gives the probability of any density profile through

$$P[\rho_A(x), \rho_B(x), \rho_C(x)] = \exp\{-N\mathcal{F}[\rho_A(x), \rho_B(x), \rho_C(x)]\} \quad (16)$$

can be written in terms of the density profiles as

$$\begin{aligned} \mathcal{F}[\rho_A(x), \rho_B(x), \rho_C(x)] = & K + \int_0^1 dx [\rho_A(x) \ln \rho_A(x) \\ & + \rho_B(x) \ln \rho_B(x) + \rho_C(x) \ln \rho_C(x)] \\ & + \beta \int_0^1 dx \int_0^1 dz [\rho_B(x) \rho_C(x+z) \\ & + \rho_C(x) \rho_A(x+z) + \rho_A(x) \rho_B(x \\ & + z)] z, \end{aligned} \quad (17)$$

where ρ_A, ρ_B , and ρ_C are periodic functions of period 1 and K is a normalization constant such that the minimum of \mathcal{F} over all profiles vanishes. The second term on the right hand side of Eq. (17) represents the entropy of the given profiles, while the term proportional to β is the continuum form of energy (15).

It is easy to derive an expression for the optimal profile for $\rho_A(x)$ by finding the extremum of Eq. (17) with respect to $\rho_A(x)$ subject to the constraint that

$$\int \rho_A(x) dx = 1/3.$$

One obtains

$$\rho_A(x) = \text{Const} \times \exp\left(-\beta \int_0^1 [\rho_B(x+z) + \rho_C(x-z)] z dz\right) \quad (18)$$

which implies that

$$\frac{d\rho_A(x)}{dx} = -\beta \rho_A(x) [\rho_B(x) - \rho_C(x)]. \quad (19)$$

Similar equations hold for $\rho_B(x)$ and $\rho_C(x)$, and using $\rho_C(x) = 1 - \rho_A(x) - \rho_B(x)$ one obtains the coupled equations

$$\frac{d\rho_A(x)}{dx} = -\beta \rho_A(x) (\rho_A(x) + 2\rho_B(x) - 1), \quad (20)$$

$$\frac{d\rho_B(x)}{dx} = -\beta \rho_B(x) [1 - 2\rho_A(x) - \rho_B(x)]. \quad (21)$$

Clearly, one solution of Eq. (20) and (21) is $\rho_A(x) = \rho_B(x) = 1/3$, which corresponds to the disordered phase, but this extremum is the minimum only in the disordered phase. To test when an ordered solution emerges, we define the Fourier series of arbitrary profiles as

$$\rho_A(x) = 1/3 + \sum_{n=1}^{\infty} [a_n \exp(i2\pi n x) + a_{-n} \exp(-i2\pi n x)], \quad (22)$$

$$\rho_B(x) = 1/3 + \sum_{n=1}^{\infty} [b_n \exp(i2\pi n x) + b_{-n} \exp(-i2\pi n x)], \quad (23)$$

$$\rho_C(x) = 1/3 + \sum_{n=1}^{\infty} [c_n \exp(i2\pi n x) + c_{-n} \exp(-i2\pi n x)]. \quad (24)$$

We insert these into Eqs. (20) and (21) and, anticipating a continuous phase transition, expand to first order in a_n, b_n . We look for values of β for which a solution for nonzero a_n, b_n, c_n is present and, therefore, the uniform solution could be unstable. One finds that the uniform solution becomes unstable to the n th mode for $\beta^2/3 = (2\pi n)^2$ so that the first instability occurs at β_c given by

$$\beta_c = 2\pi\sqrt{3} = 10.882796\dots \quad (25)$$

Near β_c , Eqs. (20) and (21) can be solved perturbatively in

$$\epsilon = \frac{\beta - \beta_c}{\beta_c}. \quad (26)$$

One finds to leading order

$$\begin{aligned}\rho_A(x) &= \rho_B\left(x + \frac{1}{3}\right) = \rho_C\left(x + \frac{2}{3}\right) \\ &= \frac{1}{3} + \left(\frac{\epsilon}{6}\right)^{1/2} 2 \cos[2\pi(x-x_0)] \\ &\quad + \left(\frac{\epsilon}{6}\right) 2 \cos[4\pi(x-x_0)] + O(\epsilon^{3/2}),\end{aligned}\quad (27)$$

where x_0 can be arbitrary (as an optimal profile remains optimal when it is translated). Also, choosing $x_0=0$, one can show that $a_n = a_{-n}$ and $a_{3m} = 0$ for $|m|=0,1\dots$ to all orders in ϵ and that to leading order in ϵ ,

$$\begin{aligned}a_1 &\sim \left(\frac{\epsilon}{6}\right)^{1/2}, \quad a_2 \sim \left(\frac{\epsilon}{6}\right), \quad a_4 \sim -\left(\frac{\epsilon}{6}\right)^2, \\ a_5 &\sim -\left(\frac{\epsilon}{6}\right)^{5/2}, \dots\end{aligned}\quad (28)$$

The parameter m defined as in Eqs. (12) and (11) becomes in the continuum limit

$$m = \int_0^1 [\rho_A^2 + \rho_B^2 + \rho_C^2] dx - \frac{1}{3},\quad (29)$$

and from Eq. (27) one obtains

$$m \sim \frac{\beta - \beta_c}{\beta_c}.\quad (30)$$

Thus, the parameter m as defined in Eqs. (12) and (11) vanishes linearly at the transition. An alternative, and probably more standard, choice for the order parameter could be the amplitude a_1 of the fundamental mode [26] and this would lead to an exponent 1/2.

We now turn to the calculation of the energy. For arbitrary density profiles, the energetic contribution to the free energy (15) may be written in terms of the Fourier coefficients as

$$E = \frac{1}{6} - \sum_{n \neq 0} \frac{a_n b_{-n} + b_n c_{-n} + c_n a_{-n}}{2\pi i n}.\quad (31)$$

For profiles $\rho_B(x) = \rho_A(x-1/3)$, $\rho_C(x) = \rho_A(x-2/3)$, this energy becomes

$$E = \frac{1}{6} - 3 \sum_{n=1}^{\infty} \frac{a_n a_{-n}}{n\pi} \sin(2\pi n/3).\quad (32)$$

Thus, using Eq. (28), near β_c we have $E \approx 1/6 - 3\epsilon/2\beta_c$ and the heat capacity $-\beta^2 \partial E / \partial \beta$ has a discontinuity of 3/2 at β_c , consistent with the data of Fig. 2.

This equal density case is similar to some special cases found in a recent study of the dynamical winding of random walks [27] for which the fact that the dynamics satisfies detailed balance allows one to write equations for the density profiles of type (20) and to locate the exact transition point.

V. NONEQUAL DENSITIES AND MEAN-FIELD THEORY

We now turn to the case of nonequal densities of particles. A direct consequence of the stochastic dynamical rules (4) is that

$$\begin{aligned}\frac{d\langle A_i \rangle}{dt} &= q\langle A_{i-1} B_i \rangle + q\langle C_i A_{i+1} \rangle + \langle B_i A_{i+1} \rangle + \langle A_{i-1} C_i \rangle \\ &\quad - q\langle A_i B_{i+1} \rangle - q\langle C_{i-1} A_i \rangle - \langle B_{i-1} A_i \rangle - \langle A_i C_{i+1} \rangle\end{aligned}\quad (33)$$

and similar equations hold for $d\langle B_i \rangle/dt$ and $d\langle C_i \rangle/dt$. We do not know how to solve these exact equations, in particular, because they require the knowledge of two point functions. One can, however, write down mean-field equations [4] by making an approximation which neglects correlations (i.e., where one replaces correlation functions such as $\langle A_{i-1} B_i \rangle$ by $\langle A_{i-1} \rangle \langle B_i \rangle$),

$$\begin{aligned}\frac{d\langle A_i \rangle}{dt} &= q\langle A_{i-1} \rangle \langle B_i \rangle + q\langle C_i \rangle \langle A_{i+1} \rangle + \langle B_i \rangle \langle A_{i+1} \rangle \\ &\quad + \langle A_{i-1} \rangle \langle C_i \rangle - q\langle A_i \rangle \langle B_{i+1} \rangle - q\langle C_{i-1} \rangle \langle A_i \rangle \\ &\quad - \langle B_{i-1} \rangle \langle A_i \rangle - \langle A_i \rangle \langle C_{i+1} \rangle.\end{aligned}\quad (34)$$

Assuming that the profiles vary slowly with i , we write $\rho_A(x) = \langle A_i \rangle$ and

$$\langle A_{i \pm 1} \rangle = \rho_A(x) \pm \frac{1}{N} \frac{\partial \rho_A(x)}{\partial x} + \frac{1}{2N^2} \frac{\partial^2 \rho_A(x)}{\partial x^2} + \dots,\quad (35)$$

then keeping leading-order terms in $1/N$ and defining $\tau = N^2 t$ in Eq. (36) yields

$$\begin{aligned}\frac{\partial \rho_A}{\partial \tau} &= \beta \frac{\partial}{\partial x} [\rho_A (\rho_B - \rho_C)] + \frac{\partial^2 \rho_A}{\partial x^2}, \\ \frac{\partial \rho_B}{\partial \tau} &= \beta \frac{\partial}{\partial x} [\rho_B (\rho_C - \rho_A)] + \frac{\partial^2 \rho_B}{\partial x^2}, \\ \frac{\partial \rho_C}{\partial \tau} &= \beta \frac{\partial}{\partial x} [\rho_C (\rho_A - \rho_B)] + \frac{\partial^2 \rho_C}{\partial x^2}.\end{aligned}\quad (36)$$

One can linearize these equations around constant density profiles

$$\begin{aligned}\rho_A(x) &= r_A + \Delta \rho_A(x), \quad \rho_B(x) = r_B + \Delta \rho_B(x), \\ \rho_C(x) &= r_C + \Delta \rho_C(x),\end{aligned}\quad (37)$$

where $\Delta \rho_A(x)$, $\Delta \rho_B(x)$, and $\Delta \rho_C(x)$ represent small departures from constant profiles at densities $r_A = N_A/N$, $r_B = N_B/N$, and $r_C = N_C/N$ (r_A, r_B , and r_C are the global densities of the three species and, of course, they satisfy $r_A + r_B + r_C = 1$). Then one finds that these small departures are damped when $\beta < \beta_c^{\text{mf}}$, given by

$$\begin{aligned}\beta_c^{\text{mf}} &= \frac{2\pi}{(2r_A r_B + 2r_A r_C + 2r_B r_C - r_A^2 - r_B^2 - r_C^2)^{1/2}} \\ &= \frac{2\pi}{[1 - 2(r_A^2 + r_B^2 + r_C^2)]^{1/2}}.\end{aligned}\quad (38)$$

We see that in the equal density case ($r_A = r_B = r_C = 1/3$), the mean-field value of β_c coincides with the exact value (25). Moreover, one finds that the solutions of the exact equations for the optimal profile (19) are steady state solutions of the mean-field equations (36) (as they make the left-hand side of these equations vanish). So, at least for the equal time properties, in this equal density case, β_c and the profiles predicted by the mean-field theory are exact.

Near β_c , one can perturbatively find stationary nonmoving profiles. The first Fourier mode of these profiles is given by

$$\Delta\rho_A(x) \simeq \psi(\epsilon) [\sqrt{r_A} e^{2i\pi(x-x_0)} + \text{c.c.}], \quad (39)$$

$$\begin{aligned}\Delta\rho_B(x) \simeq \psi(\epsilon) &\left[\frac{r_C - r_A - r_B - i\sqrt{1 - 2(r_A^2 + r_B^2 + r_C^2)}}{2\sqrt{r_A}} \right. \\ &\left. \times e^{2i\pi(x-x_0)} + \text{c.c.} \right], \quad (40)\end{aligned}$$

$$\begin{aligned}\Delta\rho_C(x) \simeq \psi(\epsilon) &\left[\frac{r_B - r_A - r_C + i\sqrt{1 - 2(r_A^2 + r_B^2 + r_C^2)}}{2\sqrt{r_A}} \right. \\ &\left. \times e^{2i\pi(x-x_0)} + \text{c.c.} \right], \quad (41)\end{aligned}$$

where ϵ is defined as in Eq. (26) and

$$\psi(\epsilon) = \frac{1 - 2(r_A^2 + r_B^2 + r_C^2)}{\sqrt{2(r_A^2 + r_B^2 + r_C^2) - 4(r_A^3 + r_B^3 + r_C^3)}} \epsilon^{1/2}. \quad (42)$$

Analyzing the whole phase diagram predicted by the mean-field equations (36) is not an easy task. Apart from the constant profile solutions, which become unstable for $\beta > \beta_c^{\text{mf}}$, other (static or moving) solutions might exist in some regions of the phase diagram and a full description of the phase diagram would require the knowledge of all the solutions of the mean-field equations and of their stabilities.

Equation (38) implies that for $r_A^2 + r_B^2 + r_C^2 > 1/2$ there is no second-order phase transition. However, looking at Eq. (42) it is clear that the second-order transition from the flat profile solution to solutions (39)–(42) should already become first order when $r_A^2 + r_B^2 + r_C^2 < 2(r_A^3 + r_B^3 + r_C^3)$. This is similar to what occurs in a mean-field study of another lattice gas [28].

At present, we cannot tell whether the predictions of the mean-field theory (36), such as Eq. (38), remain exact in the case of unequal global densities. To try to shed some light on this question, we have calculated the large deviation functional to order β^2 in a small β expansion. The details given

in the Appendix show that, in the unequal density case, the large deviation functional (16) and (17) becomes

$$\begin{aligned}\mathcal{F}[\rho_A(x), \rho_B(x), \rho_C(x)] &= K + \int_0^1 dx [\rho_A(x) \ln \rho_A(x) + \rho_B(x) \ln \rho_B(x) \\ &\quad + \rho_C(x) \ln \rho_C(x)] + \beta \int_0^1 dx \int_0^1 dz z [\rho_B(x) \rho_C(x+z) \\ &\quad + \rho_C(x) \rho_A(x+z) + \rho_A(x) \rho_B(x+z)] - \frac{3}{4} \beta^2 \\ &\quad \times \int_0^1 dx \int_0^1 dz z(1-z) [r_A(1-3r_A) \rho_B(x) \rho_C(x+z) \\ &\quad + r_B(1-3r_B) \rho_C(x) \rho_A(x+z) \\ &\quad + r_C(1-3r_C) \rho_A(x) \rho_B(x+z)] + O(\beta^3).\end{aligned}\quad (43)$$

We see that for the unequal density case, the large deviation functional is modified and terms of order β^2 appear which were not present in Eq. (17). This β^2 term is the first of a whole series in β . Without knowing these higher-order terms, it is neither possible to predict the exact value of β_c nor how Eqs. (19) and (20) for the most likely profiles would be modified. One cannot exclude the possibility that the most likely profile in the ordered phase corresponds to moving domains.

VI. CONCLUSION

In this work, we have investigated a locally driven system of three species on a ring which exhibits anomalous coarsening into a strongly phase separated steady state. In the case of equal numbers of the particles of each species, the steady state obeys detailed balance with respect to a long-range superextensive energy function, despite the strictly nearest neighbor dynamics. In the weak asymmetry regime where $q \rightarrow 1$ as in Eq. (1), one recovers an extensive energy. In this regime, we found a second-order phase transition.

For the case of equal particle densities, we have derived the large deviation (or free energy) functional (16) and (17) for the profiles. As in other examples of nonequilibrium systems studied recently [24,25], this functional is nonlocal allowing for phase transitions in one dimension. By minimizing this free energy functional, we have obtained Eqs. (19) satisfied by the optimal density profiles and analyzed the phase transition in the equal density case, in particular, we found $\beta_c = 2\pi\sqrt{3}$.

For the general case of arbitrary particle densities, we used a mean-field theory. In the case of equal particle densities, it turns out that the mean-field solution yields the same profiles as the exact free-energy optimization just discussed. An open question remains as to the extent to which the mean-field theory is valid when the densities are unequal.

The mechanism for the phase separation that we have studied can be understood through the stability of the Fourier modes of the particle densities. In the high temperature

phase, the system is disordered and the constant density profiles are stable. T_c denotes the temperature at which the lowest Fourier mode becomes unstable. As T decreases, more and more modes become unstable and the depth of the quench from the disordered high temperature phase to the low temperature phase determines the number of unstable modes which can grow from the constant profile solution. However, in the steady state one expects only three pure domains. How the nonlinear evolution of the excited modes combined with the effect of the noisy dynamics determine the anomalous coarsening [14] towards the three pure domains is another interesting open question.

APPENDIX: EXPANDING THE STEADY STATE IN POWERS OF THE BIAS

In this appendix, we justify expression (43) of the large deviation functional. Let us consider a finite system of N lattice sites and write the asymmetry q as

$$q = e^{-\phi}.$$

We are going to show in this appendix that the unnormalized weight $P(\mathcal{C})$ of a configuration \mathcal{C} in the steady state can be written to order ϕ^2 as

$$P(\mathcal{C}) = \exp[\phi R_1(\mathcal{C}) + \phi^2 R_2(\mathcal{C})], \quad (\text{A1})$$

where

$$R_1(\mathcal{C}) = -\frac{1}{N} \sum_{i=1}^N \sum_{d=1}^{N-1} d(B_i C_{i+d} + C_i A_{i+d} + A_i B_{i+d}) \quad (\text{A2})$$

and

$$R_2(\mathcal{C}) = \frac{3}{4N^2(N-1)} \sum_{i=1}^N \sum_{d=1}^{N-1} d(N-d) [N_A(N-3N_A)B_i C_{i+d} + N_B(N-3N_B)C_i A_{i+d} + N_C(N-3N_C)A_i B_{i+d}]. \quad (\text{A3})$$

In the weak asymmetry regime (1), this leads to the formula (43) in the large- N limit.

Let us try to compare two configurations \mathcal{C} and \mathcal{C}' of the form

$$\mathcal{C} = X_1 X_2 \cdots X_{i-1} A_i B_{i+1} X_{i+2} \cdots X_N, \quad (\text{A4})$$

$$\mathcal{C}' = X_1 X_2 \cdots X_{i-1} B_i A_{i+1} X_{i+2} \cdots X_N,$$

which differ only by an exchange of an A and a B particle between sites i and $i+1$ (the notation in Eq. (A4) means that site i is occupied by an A particle, site $i+1$ by a B particle, and all the other sites are occupied by arbitrary particles).

If Eqs. (A2) and (A3) were true, we would have

$$R_1(\mathcal{C}') = R_1(\mathcal{C}) - 3 \frac{N_C}{N}, \quad (\text{A5})$$

$$R_2(\mathcal{C}') = R_2(\mathcal{C}) + \frac{3}{4N^2(N-1)} \left[N_A(N-3N_A) \sum_{d=2}^{N-1} C_{i+d}(N-2d+1) - N_B(N-3N_B) \sum_{d=2}^{N-1} C_{i+d}(N-2d+1) + N_C(N-3N_C) \sum_{d=2}^{N-1} A_{i+d}(N-2d+1) - N_C(N-3N_C) \sum_{d=2}^{N-1} B_{i+d}(N-2d+1) \right]. \quad (\text{A6})$$

Using the fact that

$$C_{i+d} = 1 - B_{i+d} - A_{i+d},$$

this can be rewritten as

$$R_2(\mathcal{C}') = R_2(\mathcal{C}) + Q_A \sum_{d=2}^{N-1} A_{i+d}(N-2d+1) - Q_B \sum_{d=2}^{N-1} B_{i+d}(N-2d+1), \quad (\text{A7})$$

where

$$Q_A = \frac{3}{4} \frac{N_C(N-3N_C) + N_B(N-3N_B) - N_A(N-3N_A)}{N^2(N-1)}, \quad (\text{A8})$$

$$Q_B = \frac{3}{4} \frac{N_A(N-3N_A) + N_C(N-3N_C) - N_B(N-3N_B)}{N^2(N-1)}, \quad (\text{A9})$$

and Q_C is similarly defined. Thus, exchanging the particles at an AB interface produces in Eq. (A7) a difference between a term involving only A particles and a term involving only B particles.

Let us consider now a cluster of m sites occupied by A particles so that \mathcal{C} has the form

$$\mathcal{C} = X_1 X_2 \cdots X_i A_{i+1} \cdots A_{i+m} X_{i+m+1} \cdots X_N,$$

where sites i and $i+m+1$ are occupied by particles B or C , so that

$$X_i = L' \quad \text{and} \quad X_{i+m+1} = L'',$$

where L' is a B or a C particle and so is L'' .

There are two configurations \mathcal{C}' and \mathcal{C}'' which can be reached from \mathcal{C} by single moves at the two boundaries of this cluster. A rather simple calculation using Eq. (A6) shows that

$$\begin{aligned}
R_2(C') + R_2(C'') - 2R_2(C) &= Q_A[2mN_A - 2 - 2(m-1)N] \\
&+ Q_{L''} \sum_{d=2}^{N-1} L''_{i+m+d}(N-2d+1) \\
&- Q_{L'} \sum_{d=2}^{N-1} L'_{i+d}(N-2d+1).
\end{aligned} \tag{A10}$$

Then summing over all clusters yields

$$\begin{aligned}
\sum_{C'} [R_2(C') - R_2(C)] &= 2Q_A[N_A^2 - NN_A + (N-1)(N_{AB} \\
&+ N_{AC})] + 2Q_B[N_B^2 - NN_B + (N-1) \\
&\times (N_{BC} + N_{BA})] + 2Q_C[N_C^2 - NN_C \\
&+ (N-1)(N_{CA} + N_{CB})], \tag{A11}
\end{aligned}$$

where the sum is over all the configurations C' which can be reached from a given C by a single exchange and $N_{AB}, N_{BA}, N_{BC}, \dots$ are the numbers of neighboring pairs $AB, BA, BC \dots$ along the chain.

So far Eqs. (A5) and (A10) have been derived assuming that Eqs. (A2) and (A3) are true. To prove that Eq. (A1) does give the correct steady state weights, one needs to check stationarity, i.e.,

$$\begin{aligned}
&\left(1 - \phi + \frac{\phi^2}{2}\right)(N_{AB} + N_{BC} + N_{CA}) + N_{BA} + N_{CB} + N_{AC} \\
&= \left(1 - \phi + \frac{\phi^2}{2}\right)(N_{BA}e^{3\phi N_C/N} + N_{CB}e^{3\phi N_A/N} \\
&+ N_{AC}e^{3\phi N_B/N}) + (N_{AB}e^{-3\phi N_C/N} + N_{BC}e^{-3\phi N_A/N} \\
&+ N_{CA}e^{-3\phi N_B/N}) + \phi^2 \sum_{C'} [R_2(C') - R_2(C)]. \tag{A12}
\end{aligned}$$

This can be checked to order ϕ^2 , using simply the fact that for any configuration

$$N_{AB} - N_{BA} = N_{BC} - N_{CB} = N_{CA} - N_{AC}.$$

ACKNOWLEDGMENTS

M.C. would like to thank the Gottlieb Daimler—und Karl Benz—Stiftung, DAAD as well as EPSRC for financial support.

-
- [1] S. Katz, J.L. Lebowitz, and H. Spohn, *J. Stat. Phys.* **34**, 497 (1984).
[2] H. Hinrichsen, *Adv. Phys.* **49**, 815 (2000).
[3] J. Krug, *Phys. Rev. Lett.* **67**, 1882 (1991).
[4] B. Derrida, E. Domany, and D. Mukamel, *J. Stat. Phys.* **69**, 667 (1992).
[5] B. Derrida, M.R. Evans, V. Hakim, and V. Pasquier, *J. Phys. A* **26**, 1493 (1993).
[6] G. Schütz and E. Domany, *J. Stat. Phys.* **72**, 277 (1993).
[7] M.R. Evans, D.P. Foster, C. Godrèche, and D. Mukamel, *Phys. Rev. Lett.* **74**, 208 (1995).
[8] P.F. Arndt, T. Heinzl, and V. Rittenberg, *J. Phys. A* **31**, L45 (1998).
[9] Y. Kafri, E. Levine, D. Mukamel, and J. Török, *J. Phys. A* **35**, L459 (2002).
[10] M.R. Evans, *Europhys. Lett.* **36**, 13 (1996).
[11] B. Derrida, S.A. Janowsky, J.L. Lebowitz, and E.R. Speer, *J. Stat. Phys.* **73**, 813 (1993).
[12] K. Mallick, *J. Phys. A* **29**, 5375 (1996).
[13] M.R. Evans, Y. Kafri, E. Levine, and D. Mukamel, *J. Phys. A* **35**, L433 (2002).
[14] M.R. Evans, Y. Kafri, H.M. Koduvely, and D. Mukamel, *Phys. Rev. Lett.* **80**, 425 (1998); *Phys. Rev. E* **58**, 2764 (1998).
[15] R. Lahiri and S. Ramaswamy, *Phys. Rev. Lett.* **79**, 1150 (1997); R. Lahiri, M. Barma, and S. Ramaswamy, *Phys. Rev. E* **61**, 1648 (2000).
[16] N. Rajewsky, T. Sasamoto, and E.R. Speer, *Physica A* **279**, 123 (2000).
[17] M.E. Fisher, S. Ma, and B.G. Nickel, *Phys. Rev. Lett.* **29**, 917 (1972).
[18] F. Bernasconi, *J. Phys. (Paris)* **48**, 559 (1987).
[19] E. Marinari, G. Parisi, and F. Ritort, *J. Phys. A* **27**, 7615 (1994).
[20] M.R. Evans, *J. Phys.: Condens. Matter* **14**, 1397 (2002).
[21] K. Binder and D. W. Heermann, *Monte Carlo Simulation in Statistical Physics, An Introduction*, 3rd ed. (Springer-Verlag, Heidelberg, 1997).
[22] O.J. O'Loan and M.R. Evans, *J. Phys. A* **32**, L99 (1999).
[23] T. Tomé and A. Petri, *J. Phys. A* **35**, 5379 (2002).
[24] B. Derrida, J.L. Lebowitz, and E.R. Speer, *Phys. Rev. Lett.* **87**, 150601 (2001).
[25] B. Derrida, J.L. Lebowitz, and E.R. Speer, *Phys. Rev. Lett.* **89**, 030601 (2002).
[26] G. Korniss, B. Schmittmann, and R.K.P. Zia, *Europhys. Lett.* **45**, 431 (1999).
[27] G. Fayolle and C. Furtlehner, e-print cond-mat/0211141.
[28] I. Vilfan, R.K.P. Zia, and B. Schmittmann, *Phys. Rev. Lett.* **73**, 2071 (1994).